ADVANCED MATERIALS
www.advmat.de

Piezoelectric Biomaterials for Sensors and Actuators

Meysam T. Chorsi, Eli J. Curry, Hamid T. Chorsi, Ritopa Das, Jeffrey Baroody, Prashant K. Purohit, Horea Ilies, and Thanh D. Nguyen**

Recent advances in materials, manufacturing, biotechnology, and microelectromechanical systems (MEMS) have fostered many exciting biosensors and bioactuators that are based on biocompatible piezoelectric materials. These biodevices can be safely integrated with biological systems for applications such as sensing biological forces, stimulating tissue growth and healing, as well as diagnosing medical problems. Herein, the principles, applications, future opportunities, and challenges of piezoelectric biomaterials for medical uses are reviewed thoroughly. Modern piezoelectric biosensors/bioactuators are developed with new materials and advanced methods in microfabrication/encapsulation to avoid the toxicity of conventional lead-based piezoelectric materials. Intriguingly, some piezoelectric materials are biodegradable in nature, which eliminates the need for invasive implant extraction. Together, these advancements in the field of piezoelectric materials and microsystems can spark a new age in the field of medicine.

1. Introduction

Biomaterials are a class of natural, synthetic, alive, or lifeless materials that can interact with biological systems to augment or replace a natural function.[1] These materials should be nontoxic, noninjurious, and nonimmunogenic (i.e., also known as biocompatible) for various applications involving tissue engineering,[2–4] minimally invasive sensors,[5–7] drug delivery,[8–10] etc.

Piezoelectric materials are a family of both organic (mostly polymers) and inorganic materials that can convert mechanical force into electricity and vice versa. In inorganic piezoelectric crystals, piezoelectricity happens due to the arrangement of ions in the noninverse symmetric structure of the dielectric material.[11] The internal polarization of the material changes linearly with the applied stress, causing an electrical field to develop across the material boundary. In organic piezoelectric polymers, the piezoelectric effect is caused by the molecular structure of the polymer and its orientation.[11,12] Piezoelectricity can also be found in some mammalian tissues. For example, hair, wool, horns, and hooves are mostly composed of α-keratin with a compactly aligned and polarized α-helical structure. Most parts of the musculoskeletal tissue have a highly collagenous structure. Collagen also has a spiral structure with three helical fibrils. Each collagen fibril shows lateral piezoresponse along the fibril axis. Thus, tissues that are heavily comprised of collagen, including bone, cartilage, ligaments, and tendons, are all piezoelectric in nature.[13,14]

Among the many applications for piezoelectric technologies, those that involve interfaces with biological systems represent an exciting area of rapid development. Inorganic piezoelectric materials are biocompatible or can be biocompatible after being encapsulated. This includes materials like lead zirconate titanate (PZT),[15] aluminum nitride (AlN),[16] zinc oxide (ZnO),[17] barium titanate ($BaTiO_3$),[18] lithium niobate ($LiNbO_3$),[19] and quartz.[20] Organic materials, however, are biocompatible and environmentally friendly in nature. Polar polymers, such as polyvinylidene fluoride (PVDF), are ferroelectric and exhibit normal piezoelectric effects after poling treatments.[21] Optically active polymers, such as poly(L-lactic acid) (PLLA) and poly(D-lactic acid) (PDLA), exhibit shear piezoelectric effects after uniaxial elongation.[22,23] Devices made of piezoelectric polymers are less expensive in terms of material cost and processing, because polymer-based devices do not require advanced microfabrication facilities.[11] However, when compared to inorganic piezoelectric materials, an organic piezoelectric material often does not have a comparable piezoelectric output.[24]

All piezoelectric materials, when processed appropriately, become a powerful biomaterial that can be interfaced with

M. T. Chorsi, Prof. H. Ilies, Prof. T. D. Nguyen
Department of Mechanical Engineering
University of Connecticut
Storrs, CT 06269, USA
E-mail: horea.ilies@uconn.edu; nguyentd@uconn.edu
E. J. Curry, R. Das, J. Baroody, Prof. T. D. Nguyen
Department of Biomedical Engineering
University of Connecticut
Storrs, CT 06269, USA
H. T. Chorsi
Department of Electrical & Computer Engineering
University of California Santa Barbara
Santa Barbara, CA 93106, USA
Prof. P. K. Purohit
Department of Mechanical Engineering and Applied Mechanics
University of Pennsylvania
Philadelphia, PA 19104, USA
Prof. T. D. Nguyen
Institute of Materials Science
University of Connecticut
Storrs, CT 06269, USA
Prof. T. D. Nguyen
Institute for Regenerative Engineering
University of Connecticut Health Center
Farmington, CT 06030, USA
The ORCID identification number(s) for the author(s) of this article can be found under https://doi.org/10.1002/adma.201802084.

DOI: 10.1002/adma.201802084

biological tissues and used for miniaturized bioelectronic and biomechanical devices. In this regard, piezoelectric materials play a significant role in the field of biomedical microelectromechanical systems (BioMEMS).

The following sections provide a thorough review on different piezoelectric biomaterials that can be used in the field of biosensors and bioactuators. We will focus on the aspects of operating principles, properties, and biomedical applications. While we will discuss common piezoelectric materials used for the development of biodevices such as PVDF, PZT, ZnO, and AlN, a thorough review of organic piezoelectric materials will be provided. A comparative analysis between different organic piezoelectric materials and their most common inorganic counterparts for applications in biomedicine is also presented. We conclude with remarks on future trends and challenges of piezoelectric biomaterials for biomedical applications.

2. Mechanisms of Piezoelectricity in Inorganic and Organic Materials

2.1. Inorganic Materials

Piezoelectricity in inorganic materials is explained by displacement of ions inside crystals. When a piezoelectric material is placed under stress, the atomic structure of the crystal changes, such that the balance of ions in the structure shifts, and a dipole moment is created. For a net polarization to develop, the dipole formed must not be cancelled out by other dipoles in the unit cell. To do this, the piezoelectric atomic structure must be non-centrosymmetric, i.e., there must be no center of symmetry. Some centrosymmetric materials also experience symmetry breaking in nonequilibrium conditions or in nanoscale dimensions (e.g., hydroxyapatite) which can make them piezoelectric.[25]

Figure 1 depicts the mechanisms of piezoelectricity (process to induce polarization) for different materials. AlN is a tetrahedrally bonded semiconductor and there is a N atom in a tetrahedral interstice surrounded by four Al atoms (Figure 1a).[26] In each interstice, there is no center of symmetry, so when a stress is applied, the motion of the central atom results in a dipole moment.[27] AlN is a popular piezoelectric material for the fabrication of high frequency resonators, filters, sensors, optical devices, acousto-optic devices, surface acoustic wave (SAW) devices, and bulk acoustic wave (BAW) devices. The nontoxic AlN continues to be an attractive material for biosensors and other biodevices. AlN's widespread applications are due to numerous properties, such as chemical stability, a wide bandgap, and high acoustic velocity. Due to its high acoustic velocity and good electromechanical coupling ability,[28] the use of piezoelectric AlN thin films is in great demand for gigahertz devices and shows potential for sensor applications.

The polarization process for PZT is very similar to AlN. PZT is a non-centrosymmetric crystal structure (Figure 1b) and has a net nonzero charge in each unit cell of the crystal before the application of mechanical stress. After applying stress, there is a shift in the position of the titanium ion inside the unit cell and electrical polarity develops. As a result, the unit cell turns into an electric dipole.[15] For inorganic materials like AlN and PZT, piezoelectricity is induced by poling the material under a high electric field at an elevated temperature. For a crystalline AlN film, the piezoelectric coefficient is highly dependent on the crystal orientation of the film, which cannot be changed after deposition. In contrast, the internal dipoles of PZT can be reoriented by the application of an external electric field, leaving a remnant polarization at zero applied electric field.[11] In comparison to previously discovered metallic oxide-based piezoelectric materials, PZT exhibits greater sensitivity and has a higher operating temperature. PZT is physically strong,

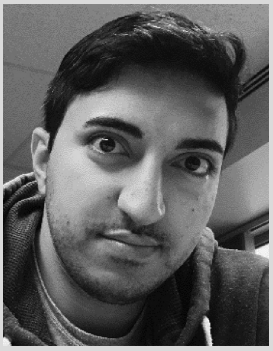

Meysam T. Chorsi received his B.S. degree in mechanical engineering from the Istanbul Technical University, Istanbul, Turkey, in 2015. He is currently working toward his Ph.D. degree in mechanical engineering at the University of Connecticut, Storrs, CT, USA. His research interests include biomaterials, protein-based biodevices, and biosensors.

Eli J. Curry is currently pursuing his Ph.D. in biomedical engineering at the University of Connecticut. He also received his B.S. in biomedical engineering at the University of Connecticut (2016). His doctoral research is on the development of novel, biodegradable, piezoelectric devices for use in sensing and tissue regeneration applications.

Thanh D. Nguyen is currently an assistant professor of mechanical engineering and biomedical engineering at the University of Connecticut. He received his Ph.D. in mechanical engineering at the Princeton University (2013), and performed his postdoctoral training at the Koch Institute, Massachusetts Institute of Technology (MIT, 2013–2015). His current research is focused on the transformation of biopolymers into "smart" materials with novel 3D structures at small scales for applications in tissue engineering, control drug delivery, and medical devices.

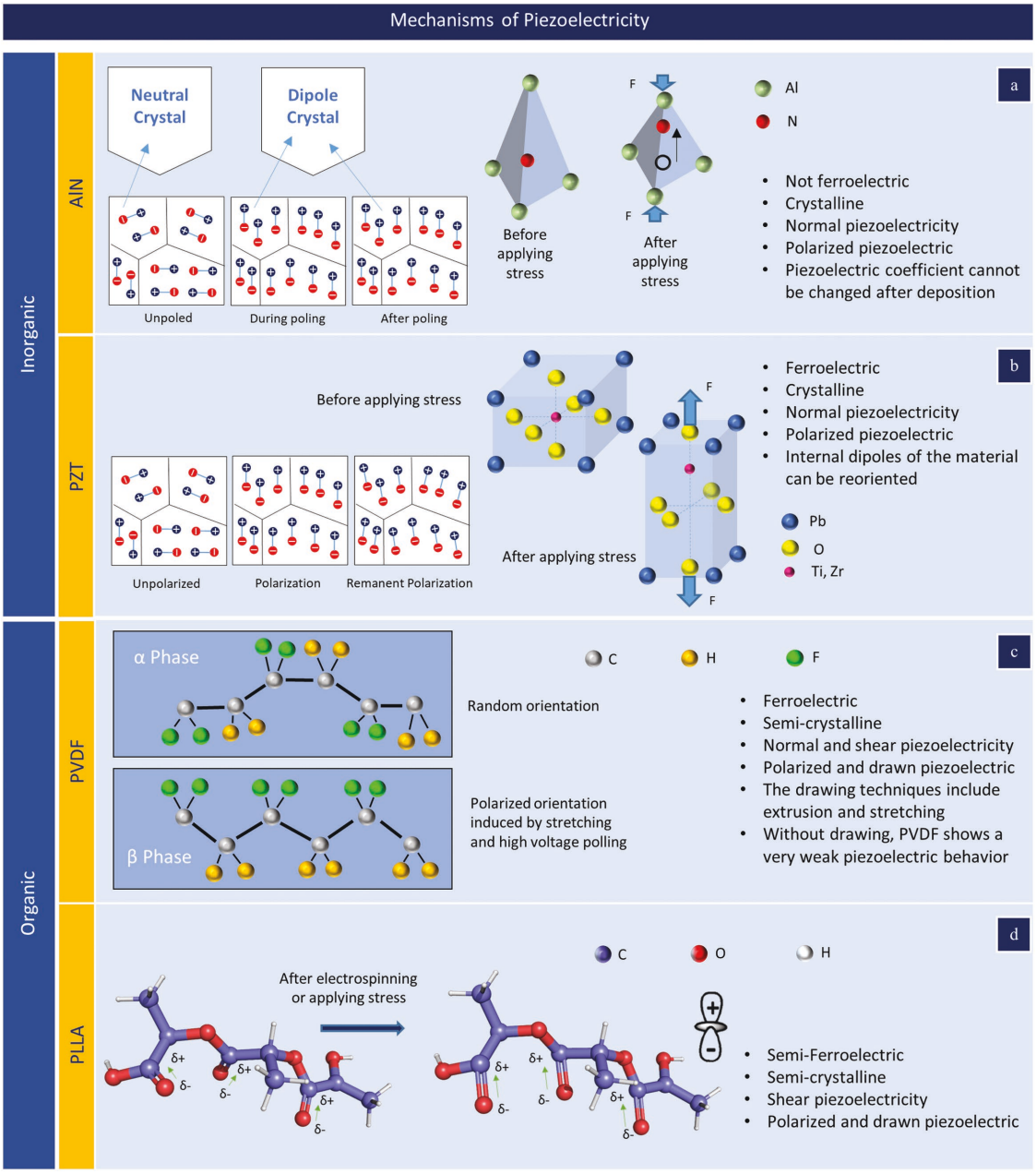

Figure 1. Mechanisms of piezoelectricity in different materials. a) Polarization process of AlN[60] and the effect of piezoelectricity on the tetrahedral coordinate of a AlN crystal. b) Polarization process of PZT[61] and stress-induced phase transition in PZT.[15] c) Structures of non-piezoelectric (α-phase) and piezoelectric (β-phase) PVDF.[49] d) Molecular structure of PLLA chain with orientation of C=O dipoles in all directions and preferential orientation of the C=O dipoles after electrospinning process.[57]

chemically inert, and relatively inexpensive to manufacture.[29,30] PZT possesses superior electromechanical properties, owing to its large piezoelectric charge constant, rendering it particularly attractive for applications in biodevices.[31] Although PZT and inorganic materials possess inferior flexibility when compared to their organic counterparts, many inorganic materials assembled in ultrathin films or nanowires (NWs) can exhibit good mechanical flexibility.[32–34]

Biocompatibility is essential for the application of biosensors in vivo or in vitro. Biocompatibility must be investigated for PZT, mostly due to the fact the material contains lead, which adversely effects organisms.[35] Some researchers have attempted to transform PZT into a piezoelectric ceramic with excellent biocompatibility. In one example, researchers tried to improve the biocompatibility of PZT by treating the surface with titanium, which has a high biocompatibility and has been used extensively in orthopedic metallic implants.[36] The results indicate that the proliferation rate of titanium-coated PZT is good, but different approaches such as dipping a metal into blood are still required. Perovskite piezoelectric materials, aside from PZT, such as $BaTiO_3$-, $LiNbO_3$-, lead zirconate niobate–lead titanate (PZN–PT)-, lead magnesium niobate–lead titanate

(PMN–PT)-, barium zirconate titanate–barium calcium titanate (BZT–BCT)-, potassium sodium niobate (KNN)-, and bismuth sodium titanate (BNT)-based materials are also biocompatible.

ZnO is an inorganic piezoelectric material and has a unique set of properties including excellent transparency,[37] high electron mobility,[38] and biocompatibility.[39] ZnO can also be used for flexible mechanical energy harvesting devices and as an active material for transient electronics and strain sensing devices.[40,41] Although zinc oxide has many advantages, very high processing temperatures are required to fabricate ZnO-based devices (400–500 °C)[42] which limits its application to some specific areas.

Gallium nitride (GaN) is a biocompatible piezoelectric material.[43] Additional advantages of GaN include a large energy bandgap of 3.4 eV,[44] high electron mobility,[45] excellent chemical stability,[46] and low electrical drift in ionic solutions.[47] Gallium nitride provides no biofunctional influence on cellular environments,[48] which is an important parameter for future biosensing applications.

2.2. Organic Materials

Piezoelectricity in organic materials is the process of reorienting the molecular dipoles within the bulk polymer. This can be achieved through the application of a high electrical field or stretching (drawing). Other organic piezoelectric materials like glycine, collagen, silk, self-assembled diphenylalanine peptide nanotubes (PNTs), and graphene have also attracted attention in recent years.

Figure 1c depicts this process for PVDF. Five crystal phases (α, β, γ, δ, ε) have been reported for PVDF, and α and β phases are the most commonly utilized.[49] In the α phase, the chains are packed in the unit cell so that the molecular dipoles are antiparallel, resulting in nonpolar crystal structures. The β phase exhibits the best piezoelectric properties, because all the dipoles are parallel and contribute to the highest dipole moment per unit cell.[50] Unlike other piezoelectric materials, such as PZT, PVDF has a negative d_{33} value. This negative piezoelectric effect arises from the self-consistent quantum redistribution of electron molecular orbitals, the shifting of charged atomic nuclei, and dipole reorganization, under the action of applied electric field.[51] Physically, this means that PVDF will compress when exposed to the same electric field that makes PZT expand.[52] The negative piezoelectric effect could be useful for new applications in biosensing and energy harvesting. The inertness of PVDF makes it a good candidate for use in surgical meshes and sutures, while its piezoelectricity makes it an appropriate material for wound healing.[53] Attempts have been made to use PVDF together with other materials to form composites that would overcome such drawbacks.[54–56]

Figure 1d (left) presents PLLA in the α-crystalline form (thermodynamically stable conformation), where the C=O dipoles are randomly oriented along the main chain. In order to induce piezoelectricity, the chains must be thermally stretched to transform the α-crystalline form into β-crystalline form, which represents a change from randomly oriented molecular chains to molecular chains being aligned along the stretched direction.[57] The electrospinning process can also align the C=O bond to create piezoelectric PLLAs as seen in Figure 1d (right). PLLA is a transparent and very flexible plant-derived polymeric material, and is considered suitable for applications in mobile devices as an environmentally friendly, flexible, transparent, piezoelectric thin film.[58] However, the practical application of PLLA is limited because its piezoelectric constant is much lower than that of inorganic piezoelectric materials such as PZT. It is noted that elongated PLLA films have no spontaneous polarization, unlike poled polymers such as PVDF, but still have a large shear piezoelectric constant.[59] Although it has a complex higher ordered structure with intermingled crystalline and amorphous regions, it is possible to control the degree of crystallinity of PLLA through a thermal annealing process. Therefore, the piezoelectric constant of a PLLA film can be engineered and improved by increasing crystallinity and molecular orientation. This biodegradable and biocompatible film has many promising applications in the future of biosensors/actuators.

Glycine is a polymorphic amino acid and can form three distinct crystalline structures (α, β, and γ structures) depending on the crystallization conditions.[62] α-glycine is centrosymmetric, and thus non-piezoelectric.[63] β- and γ-glycine have acentric structures and generate shear piezoelectricity.[64] The piezoelectric strain constant and piezoelectric voltage constant of β-glycine was measured to be around $d_{16} = 190$ pm V^{-1} and $g_{16} = 8$ Vm N^{-1}, respectively.[63] This high piezoelectricity along with the biocompatibility and controllable biodegradability of glycine makes this piezoelectric, organic material potentially useful for biomedical and biotechnological applications.

The piezoelectric effect in collagen comes from polar and charged groups in the molecule.[65] Under mechanical stress, the dipole moments of these residues reorient toward the long axis of the collagen molecule and the magnitude of the dipole moments change. Together, these effects result in the overall piezoelectric effect in collagen.[65] The shear piezoelectric constant of collagen is around $d_{14} = 0.1$ pm V^{-1},[66] but recent studies tend to improve this value by adding chitosan[67] or by adjusting the pH from acidic to neutral.[68]

Silk is known to have a combination of amorphous and crystalline phases.[69] Silk's piezoelectricity is due to a combination of a high degree of silk II, β-sheet crystallinity, and crystalline orientation.[70] Silk films with draw ratio = 2.7 exhibit shear piezoelectric coefficients of $d_{14} = -1.5$ pC N^{-1}.[70] Silk fibroins have found their use in tissue engineering,[71] regenerative medicine,[72] and bone fracture healing.[73] Piezoelectric silk could potentially enable development of exciting piezoelectric silk-based BioMEMS devices/wearable sensors.

Self-assembled PNTs also show shear piezoelectricity.[74,75] PNTs are made from amino acids, and are very promising candidates for the future generations of "green" piezoelectric materials and piezodevices. The shear piezoelectric constant of PNT is around $d_{15} = 60$ pm V^{-1}.[74]

Biomedical applications of 2D materials like graphene are rapidly growing.[76–78] Recent discovery of the piezoelectric effects in graphene[79] has opened a new avenue for piezoelectric sensors and actuators due to the unique properties of these materials such as high flexibility and stretchability.

New classes of composite piezoelectric materials tend to combine different advantages of inorganic materials (e.g., high piezoelectricity) and organic materials (e.g., flexibility). Recent

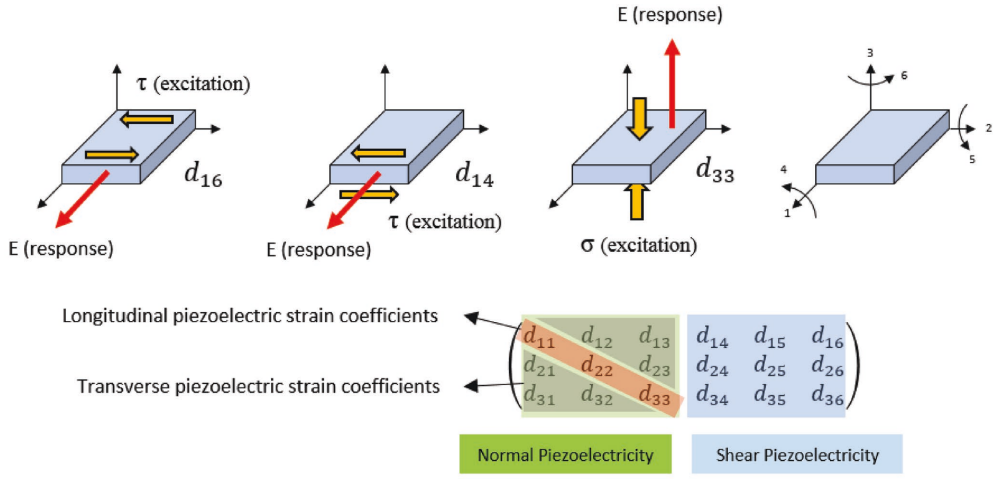

Piezoelectric Biomaterial	Material Type	Piezoelectric Constants	Refs.
PZT-5H	Anisotropic (Orthotropic), Ceramic	d_{33}= 593 [pC/N], d_{31}= -274 [pC/N]	[84]
AlN	Anisotropic, Ceramic	d_{33}= 3-6 [pC/N], d_{31}= -2 [pC/N]	[85]
Quartz	Anisotropic (Orthotropic), Single Crystal	d_{11}= 2.3 [pC/N], d_{14}= -0.67 [pC/N]	[86]
ZnO	Anisotropic, Crystal	d_{33}= 6-13 [pC/N], d_{31}= -5 [pC/N]	[87]
$BaTiO_3$	Anisotropic (Orthotropic), Ceramic	d_{33}= 190 [pC/N], d_{31}= -78 [pC/N]	[86]
$LiNbO_3$	Anisotropic (Orthotropic), Ceramic	d_{33}= 16 [pC/N], d_{31}= -1 [pC/N]	[86]
PMN-PT	Anisotropic, Single Crystal	d_{33}= 2000-3000 [pC/N]	[87]
GaN	Anisotropic, Crystal	d_{33}= 2-4 [pC/N], d_{31}= -1.5 [pC/N]	[85]
PVDF	Anisotropic, Polymer	d_{33}= -33 [pC/N], d_{31}= 23 [pC/N]	[87]
PLLA	Anisotropic (Transversely Isotropic), Polymer	d_{14}= 6-12 [pC/N]	[88]
β-Glycine	Anisotropic, β-Crystal	d_{16}= 195 [pm/V]	[63]
Collagen	Anisotropic, Non-oriented	d_{14}= 0.1 [pm/V]	[66]
Silk	Anisotropic, Semi-crystalline, Draw Ratio=2.7	d_{14}= -1.5 [pC/N]	[70]
Peptide Nanotubes	Self-assembly process of diphenylalanine	d_{15}= 60 [pm/V]	[74]
Graphene	Single-layer	d_{33}= 1.4 [nm/N]	[79]

Figure 2. Relationship between applied normal (σ) and shear (τ) stress and corresponding induced electric field (E), and comparison of piezoelectric coefficients for different biocompatible piezoelectric materials.

developments in piezoelectric nanocomposite–based biomedical devices have shown various applications for these materials.[80–82] Organic–inorganic hybrid nanogenerators are very promising for various applications ranging from flexible wearable electronics to human–machine interfaces.[81,83]

Figure 2 provides a comparison of piezoelectric coefficients for different biocompatible piezoelectric materials.

3. Device Applications from Different Piezoelectric Materials

3.1. Applications of Inorganic Piezoelectric Materials

3.1.1. Cell and Tissue Characterization

Nanoribbons of PZT have been developed by Dagdeviren et al.[89] that enable in vivo measurements of soft tissue viscoelasticity. The device is made by a stacking and microcontact transferring method (**Figure 3**a). An array of actuators is laminated on the skin and stimulated to generate tissue deformations that are measured by another set of the PZT sensors to provide information on the mechanical properties of skin (Figure 3b). Unlike conventional characterization methods which are invasive and tailored only for specific regions of the body, their systems achieved conformal contact with the underlying complex topography and texture of the targeted skin. The group then validated their piezoelectric actuator–sensor pairs by applying them on a variety of soft biological tissues and organ systems in animal models. Figure 3c–f shows the ex vivo measurements from the apex of the bovine heart, left ventricle (LV) and right ventricle (RV), and lung. Studies on human subjects established the clinical significance of these devices for rapid and noninvasive characterization of skin mechanical properties.

In another work, Nguyen et al.[90] used PZT nanoribbons to measure mechanical deformations generated by cells and tissues. They transferred arrays of PZT nanoribbons onto a silicone elastomer and measured mechanical deformations of an explanted cow lung during simulated respiration (Figure 3g,h). The PZT nanoribbons provide a minimally invasive and scalable stage for electromechanical biosensing. Yet, work to investigate the long-term biocompatibility of the PZT nanoribbons in vivo should be performed prior to the use of these PZT-based devices in the human body.

3.1.2. Energy Harvesting

Piezoelectric energy harvesting systems are promising for use in future self-powered biomedical electronics. Recently, various kinds

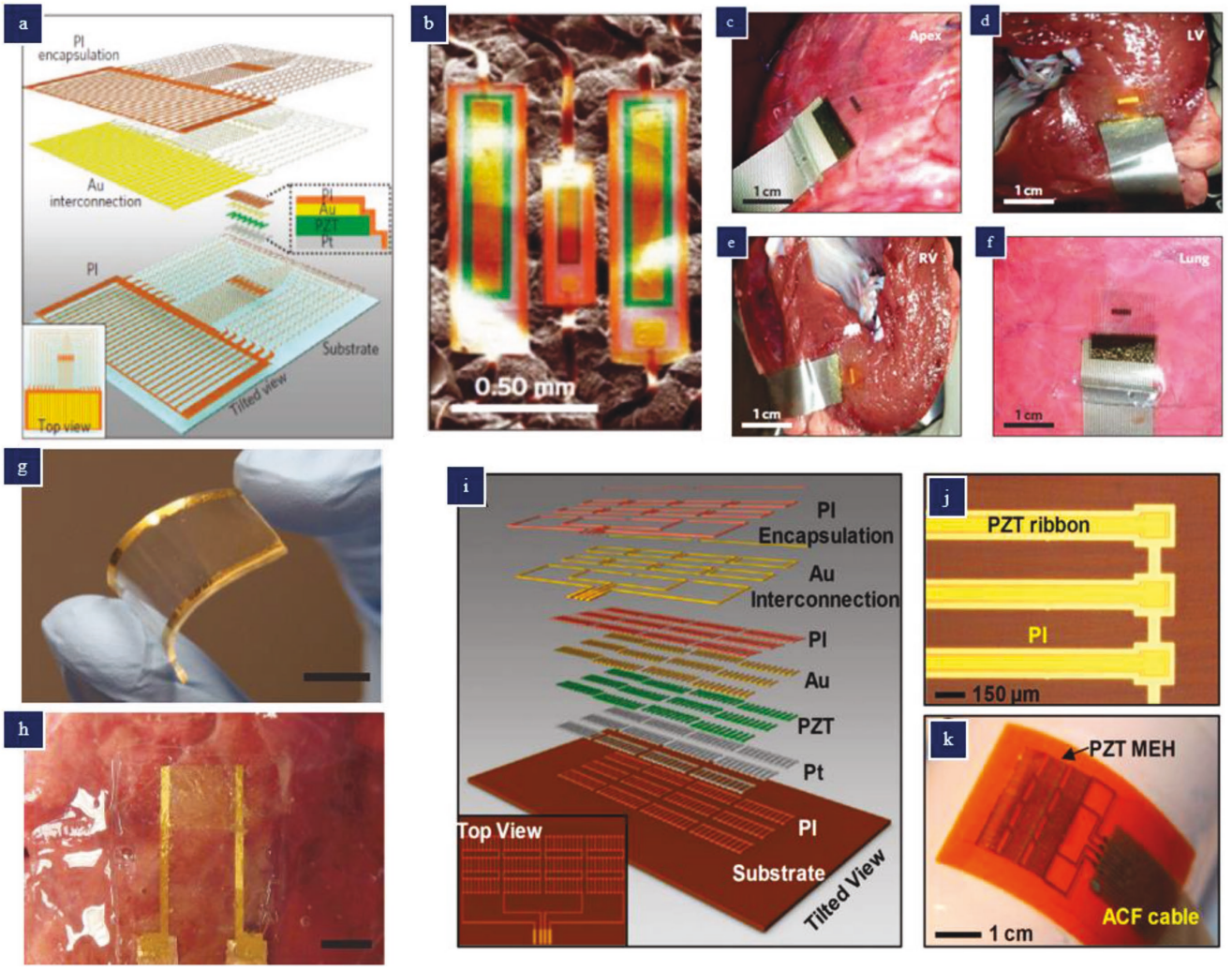

Figure 3. Applications of inorganic piezoelectric materials. a–f) Compliant modulus sensor (CMS)–based on nanoribbons of PZT in arrays of mechanical actuators and sensors. (a) Exploded-view schematic illustration of the device, with a top view in the lower-left inset, and a cross-sectional view of actuators and sensors in the black-dashed inset. (b) SEM image of a device on an artificial skin sample. (c–f) Photographs of a device placed on: (c) heart apex, (d) left ventricle, (e) right ventricle, (f) lung. a–f) Reproduced with permission.[89] Copyright 2015, Nature Publishing Group. g,h) Piezoelectric nanoribbons for monitoring cellular deformations. (g) Photograph of flexible PZT nanoribbon chip. (h) Photograph of PZT nanoribbons on PDMS biointerfaced with cow lung tissue for sensing deformations during a mimicked respiration process. g,h) Reproduced with permission.[90] Copyright 2012, Nature Publishing Group. i–k) Flexible PZT mechanical energy harvester (MEH). (i) Exploded-view schematic illustration with a top view (inset). (j) Optical microscopy image of PZT ribbons printed onto a thin film of PI. (k) Photograph of a flexible PZT MEH with cable for external connection. i–k) Reproduced with permission.[91] Copyright 2014, National Academy of Sciences.

of piezoelectric materials such as PZT, PMN–PT, ZnO, and $BaTiO_3$ have been utilized to scavenge energy from various sources of deformation, including body movements and heartbeats.

Dagdeviren et al.[91] worked on a flexible PZT-based energy harvester that is capable of storing energy from the natural motions of the heart, lung, and diaphragm. A thin layer of Au/Cr (gold/chromium) was deposited on the top of PZT ribbons as an electrode. The bottom platinum/titanium (Pt/Ti) electrode was patterned by a wet etching process and then the device was sealed with a poly(dimethylsiloxane) (PDMS) stamp. A schematic, an optical microscope image, and a photograph of the device are illustrated in Figure 3i–k. In vivo testing involved attaching the device to the RV, LV base, and free wall of bovine and ovine hearts. The results showed that the piezoelectric energy harvester can store significant electrical power from motions of internal organs at levels that meet requirements for practical applications.

Hwang et al.[92] fabricated a self-powered cardiac pacemaker by single crystalline PMN–PT. Top and bottom Au electrodes are deposited on both sides of the PMN–PT film using DC sputtering. A layer of SU-8 was then coated on the PMN–PT energy harvester to protect the device. The animal experiment was conducted to implant the energy harvester in the cardiac muscle of a live rat to detect deformations from the heart and power the pacemaker. The reported results describe a high electric power that can be used as an additional energy source for a pacemaker.

Nanogenerators based on other piezoelectric materials such as ZnO and GaN have also been studied to harvest the biomedical energy.[93–96] Flexible, bendable, and stretchable ZnO

nanowires and GaN nanorods are promising for solving power supply problems in biomechanical devices because they can maintain high performance under strain and deformation.

3.1.3. Biochemical Sensing

Some specific biomolecules and proteins can be detected through piezoelectric biosensors. Piezoelectric materials with high acoustic velocity are a very good candidate for this application. AlN piezoelectric acoustic biosensors provide real-time responses and quantified data.[97,98] Chen et al.[98] developed a highly sensitive AlN biosensor and used it to detect pesticide residues. On one of the faces of the piezoelectric resonator, acetylcholinesterase enzyme is attached as the sensitive coating. From the reduction of the frequency shift compared with the levels found in their absence, traces of organophosphorus pesticides in the solution can be detected. The AlN biosensor exhibits a remarkably low detection limit, a linear response, and good reproducibility. This method can be extended to detect a wide variety of biological reactions, such as antigen–antibody binding, protein–ligand interactions, and genetic hybridizing, which could provide information for the studies of biological reaction kinetics.

3.2. Applications of Organic Piezoelectric Materials

3.2.1. Pressure Sensing

Organic piezoelectric materials are more flexible than their inorganic counterparts, therefore they can deform under smaller applied forces. This behavior makes them suitable for biomedical pressure sensing applications.

Aligned nanofibers of PVDF have been used by Persano et al.[99] to fabricate a flexible, self-powered, and lightweight pressure sensor. Polyimide substrates are attached to the ends of a ribbon shaped sample of fiber arrays, as depicted in **Figure 4**a. Figure 4b shows the freestanding film of highly aligned PVDF–trifluoroethylene (TrFE) fibers. The result of a cyclic bending test is presented in Figure 4c. This device is capable of measuring small pressures (≈0.1 Pa). The collective results suggest that the capabilities of the sensor could be valuable for a range of applications in biomedical and wearable electronics.

Biodegradability is an essential element for the detection of molecules in the next-generation of biosensors. In some acute or short-term medical applications (e.g., wound or bone healing), where sensor functionality is required only for a limited time, the implantation of biodegradable PLLA sensors could avoid the need for a secondary removal surgery.

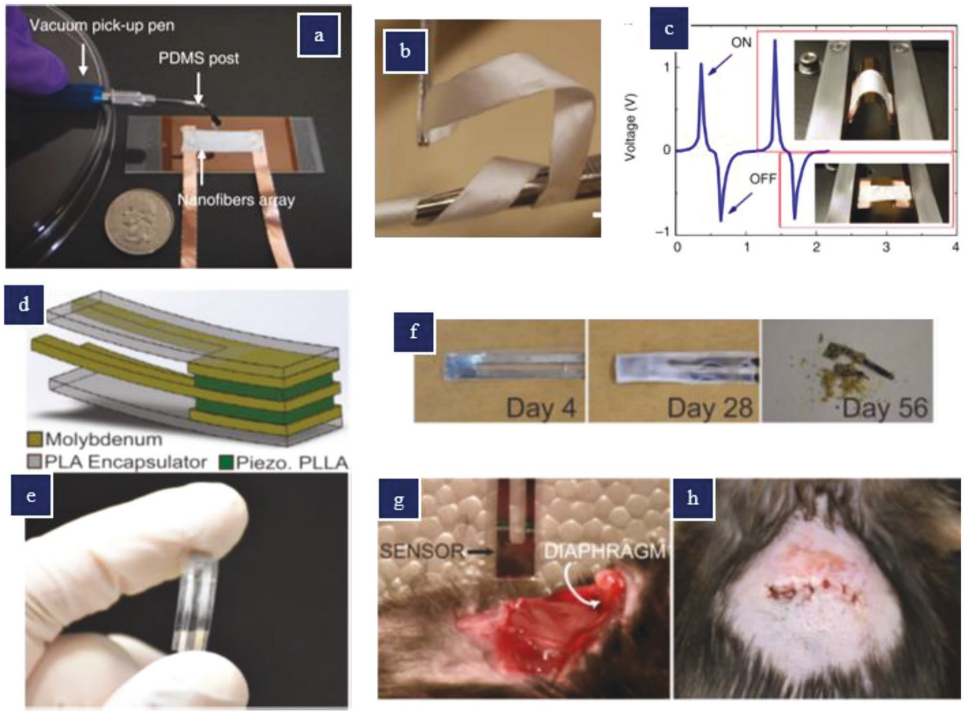

Figure 4. Organic piezoelectric materials for pressure sensing. a–c) Piezoelectric PVDF pressure sensor. (a) Photograph of the manipulator used to apply pressures, for the purpose of studying the voltage response. (b) Photograph of a freestanding film of highly aligned piezoelectric fibers. Scale bar, 1 cm. (c) Measured voltage response of an array of PVDF–TrFe fibers under cycling bending at 1 Hz. a–c) Reproduced with permission.[99] Copyright 2013, Nature Publishing Group. d–h) Biodegradable piezoelectric PLLA pressure sensor. (d) Simplified schematic representing the biodegradable piezoelectric PLLA sensor. (e) Optical image of a fabricated biodegradable piezoelectric PLLA sensor. (f) Optical images showing the sensor at different days in the buffered solution. (g) Optical image illustrates the sensor and a mouse abdominal cavity with diaphragmatic membrane. (h) Surgical wound closed up by medical suture on abdomen of the mouse, which received an implanted PLLA sensor. d–h) Reproduced with permission.[100] Copyright 2018, National Academy of Sciences.

The first completely biodegradable piezoelectric force sensor was developed by Curry et al.[100] to monitor important physiological forces. Piezoelectric PLLA is made by a stretching/annealing process at 90 °C for 8 h. A 3 mm × 15 mm patch of treated PLLA was cut at a 45° angle relative to the stretched direction of a draw ratio 4.6 film to fabricate the piezoelectric element of the sensor. A combination of magnesium/iron is deposited on the film and the film is then folded and compressed between molybdenum electrodes to achieve a multilayer design depicted in Figure 4d. The sensor is then compressed between sheets of 100 µm thick poly(lactic acid) (PLA), and sealed with biodegradable PLA glue and a thermal bag sealer. This results in the biodegradable PLLA sensor depicted in Figure 4e. As depicted in Figure 4f, the sensor is completely degraded after a period of 56 days at an elevated temperature of 74 °C. Due to the sensor's ability for miniaturization and the biocompatible/biodegradable nature of the materials used, it can be implanted anywhere in the body with minimal immune response. For instance, the group demonstrated the PLLA piezosensor can be implanted inside the abdominal cavity of a mouse to monitor the pressure of diaphragmatic contraction (Figure 4g,h). The device has a wide range of measurable pressures (0–18 kPa). Moreover, the simple fabrication process, compared to photolithography-based sensors, makes the sensor more promising for clinical implementation.

3.2.2. Catheter Applications

PVDF has been studied recently as a sensing element in endovascular catheters due to its flexibility, stretchability, and biocompatibility.[101–105] In a notable example,[105] PVDF–TrFE core–shell nanofibers are fabricated using poly(3,4-ethylenedioxythiophene) (PEDOT) (a conducting polymer) as a core and PVDF–TrFE as a shell (**Figure 5**a). A thin film of copper is deposited to create the external electrode. Highly aligned nanofibers were fabricated to significantly boost device sensitivity and flexibility (Figure 5b). The fabrication process of this electrospun-nanofiber-based sensor is presented in Figure 5c. The results show that core–shell fiber-based device has significantly boosted the sensitivity, nearly 40-fold higher than the thin-film structures.

PVDF-based sensors have been used by Sharma et al.[102] to measure the real-time flow in catheter applications. This is accomplished by spin-coating PVDF–TrFE copolymer into thin films to tap the near β-phase formation. The biocompatible PVDF–TrFE sensor is fabricated using low-cost, low-temperature fabrication techniques (Figure 5d),

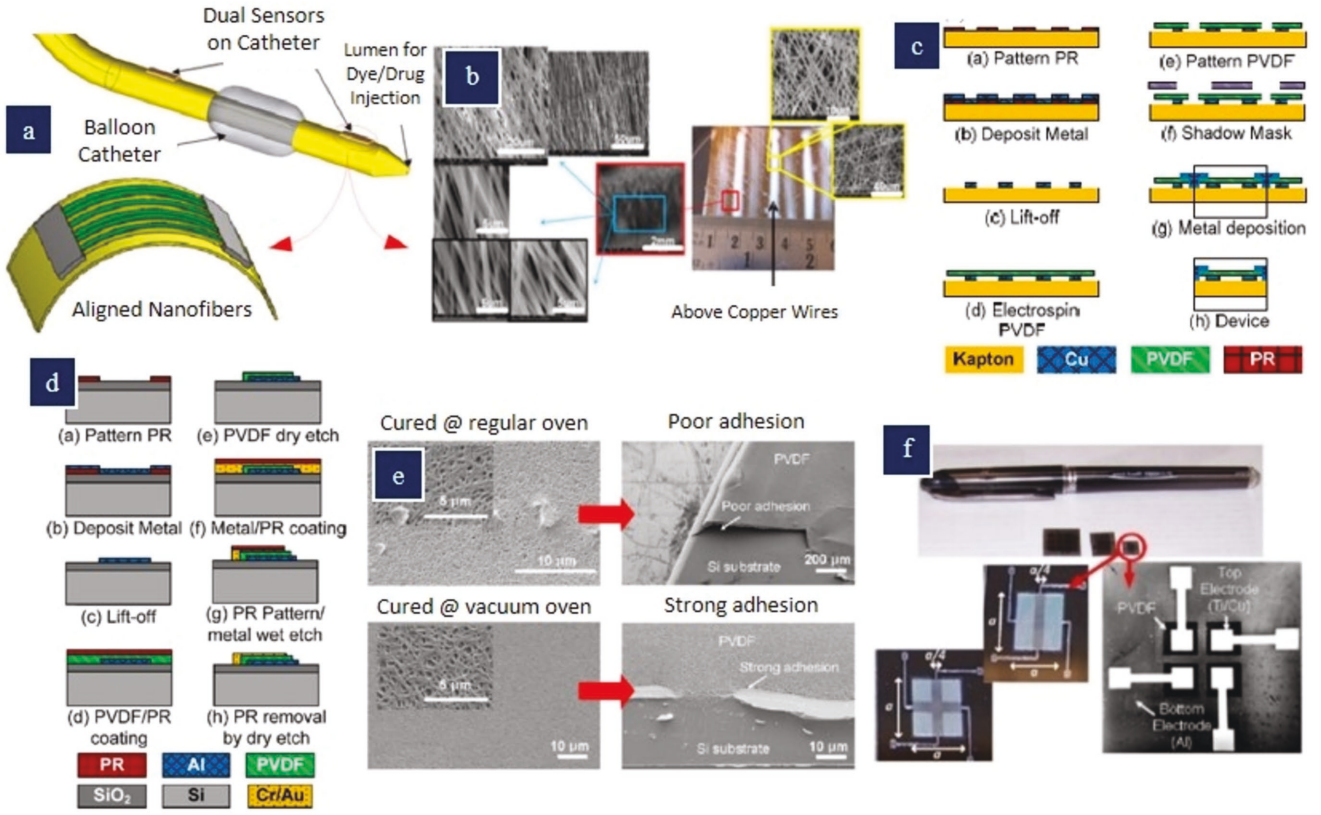

Figure 5. Organic piezoelectric materials for catheter application. a) Smart catheters with PVDF nanofiber–based pressure sensors. b) Photograph and SEM images showing patterned nanofibers in aligned and random orientations. c) Schematic for fabrication of electrospun nanofiber–based devices. a–c) Reproduced with permission.[105] Copyright 2013, IEEE. d) Fabrication process for PVDF–TrFE devices. e) SEM images of PVDF–TrFE thin film on substrate. f) Fabricated metal–PVDF–TrFE–metal (MIM)-structured pressure sensors of dual and quadruple membrane devices (bottom half) showing the device dimensions. d–f) Reproduced with permission.[102] Copyright 2012, Elsevier.

and is later integrated with a catheter for intravascular measurements. The process is fully compatible with existing micromachining fabrication processes without additional mechanical stretching and electrical poling. Different ratios of PVDF–TrFE and curing processes are studied to find the optimum conditions for better adhesion (Figure 5e). They show that a thinner PVDF film (1 µm) shows higher piezoelectricity and sensitivity than a thicker film (6 µm). This sensor (Figure 5f) demonstrated great potential for flow direction measurements as an implantable biomedical device owing to its fast recovery time (0.17 s), biocompatibility, and compact form factor. Piezoelectric PVDF nanofibers have shown great promise for the realizations of more robust, reliable, flexible sensors on catheters to revolutionize the field of minimally invasive surgeries.

3.2.3. Healthcare Monitoring

Over the last few years, noninvasive biosensors demonstrated unique capabilities for physiological signal monitoring, disease diagnosis, and health assessment. Electronic skins (e-skins) with their flexible and stretchable properties have attracted increasing attention for potential applications in wearable sensors, medical diagnostic devices, and healthcare monitoring systems.

Flexible ferroelectric skins, fabricated by composite films of PVDF and graphene oxide (GO), were used to detect and discriminate between multiple stimuli, including static/dynamic pressure, and temperature, with high sensitivities. PVDF/GO films were cast at 50 °C to crystallize the PVDF into β-phase, and then annealed at 160 °C to increase the conductivity, and finally quenched in liquid nitrogen. Schematic diagrams of the sensor array are depicted in **Figure 6**a. By placing gold electrode arrays on the top and bottom of the film, the temperature variation of a human hand can be mapped by the temperature sensor (Figure 6a). Figure 6b shows the ability of the e-skin to monitor the simultaneous artery pulse pressures and temperature. Flexible, stretchable, and cost-effective wearable e-skins are promising tools for the prevention of illnesses and the prediction of early diseases.

In another work, a wearable self-powered PVDF sensor is fabricated by Liu et al.[106] for respiration sensing and healthcare monitoring. The structure of the piezoelectric sensor is illustrated in Figure 6c. Gold films are employed as electrodes to compactly sandwich both the surfaces of the compressed PVDF film and a silicone substrate is used to enhance the flexibility of the whole device. The sensor has been placed in different parts of body for different pressure sensing applications. It can be used as a physiological signal recording system to measure respiration signals, or as a detector for human gestures and vocal cord vibrations. Since the piezoelectric sensor can detect subtle muscle movements, it has promising applications in the recovery of stroke patients who have suffered paralysis.

Human physiological monitoring systems based on other piezoelectric materials such as silk[69,107] and collagen[108,109] have also been studied recently (Figure 6d,e). A flexible/wearable electronic device based on natural silk[69] and a fish skin–based electronic skin composed of collagen nanofibrils[108] are other notable developments in personalized healthcare monitoring systems.

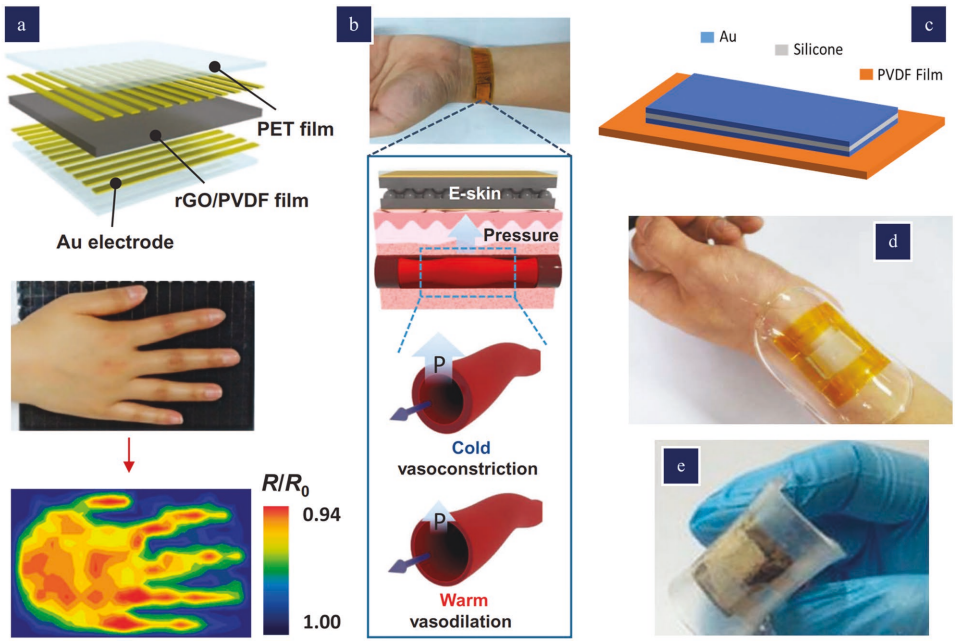

Figure 6. Organic piezoelectric biomaterials for healthcare monitoring. a,b) Human-skin-inspired multifunctional e-skin. a) Detection of temperature distribution on the human palm. b) Photograph of a wearable e-skin for monitoring artery pulse pressure and temperature. The enlarged schematic illustrations indicate the effect of temperature on the constriction (cold) and dilation (warm) of arterial vessels. a,b) Reproduced with permission.[110] Copyright 2015, Science Publishing Group. c) Structure of the wearable PVDF electrospun sensor for health monitoring. d) Photograph of the silk device for detection of wrist pulses. Reproduced with permission.[107] Copyright 2014, Wiley-VCH. e) Photograph of the collagen-based flexible sensor. Reproduced with permission.[108] Copyright 2017, American Chemical Society.

3.2.4. Cell and Tissue Actuators

PVDF: Tissue stimulators that are biocompatible, biodegradable, small, and flexible have been used in various biomedical applications. Several studies have shown that organic piezoelectric actuators, for example, PVDF can be used for tissue engineering scaffolds to promote tissue regeneration.

Frias et al.[111,112] used a PVDF actuator to experimentally validate the use of piezoelectric materials as a means of directly straining bone cells by the converse piezoelectric effect. The actuator consists of a thin film of PVDF, printed with silver ink on both sides as electrodes (**Figure 7**a). The PVDF surface is coated with poly(methyl methacrylate) (PMMA)/bone-like apatite layer to improve adhesion of osteoblasts to the device surface and electrical insulation (Figure 7b,c). Osteoblasts were grown on the surface of the piezoelectric material and the cellular response of the osteoblasts was studied. These results suggest that the both static and dynamic substrates affect cell viability and proliferation.

Damaraju et al.[113] showed that piezoelectric materials can be fabricated into flexible, 3D fibrous scaffolds and can be used to stimulate human mesenchymal stem cell differentiation. Figure 7d,e shows the testing device used to measure the electrical output from the bulk scaffold. Figure 7g,h illustrates the electrospun piezoelectric scaffolds and the annealed PVDF–TrFE fibers, respectively. Piezoelectric scaffolds that exhibit high output voltage helped osteogenic differentiation. On the other hand, piezoelectric scaffolds with a low voltage output helped chondrogenic differentiation. Results show that cell differentiation under electromechanical actuation is greater than mechanical actuation alone.

Piezoelectric nanocomposites using PVDF fibers and barium titanate nanoparticles (BTNPs) are investigated by Mota et al.[114] for cochlear stimulation. BTNP/PVDF ultrafine fibers were electrospun and used as novel electromechanical transducers to restore cochlear function. To explore the biocompatibility of the material, OC-k3 epithelial cells were seeded into wells containing nanocomposite fibers (Figure 7i). The epithelial cells showed intact nuclei in the areas surrounding the fibers, thus indicating their cytocompatibility (Figure 7j). The BTNP/PVDF fibers also promoted the proliferation of neural cells under dynamic culture (Figure 7k,l). Collectively, the obtained findings are highly suggestive that nanostructured piezoelectric materials will be able to improve the material performance by favoring the tissue/material interaction at targeted cellular levels.

The effect of electrospinning parameters on the piezoelectricity of PVDF nanofiber actuators is investigated by Wang et al.[115] PVDF nanofibers were fabricated using an electrospinning setup and then were pressed to get a smooth surface. The pressed fibrous mat was sputtered with Au electrodes on both the surfaces and then poled in a silicon oil bath under an electric field to obtain high piezoelectricity (Figure 7m). The fabricated actuator under optimized electrospinning conditions was then used for implanted energy harvesting in rats (Figure 7n). Since electrospun PVDF–TrFE nanofibers have excellent biocompatibility and a large piezoelectric effect, fibroblast cells developed perfectly along the fiber direction, and the proliferation rate was promoted by 1.6-fold (Figure 7o,p).

Using wireless stimulations to induce piezoelectricity in polymers to promote differentiation of neuronal cells can create a new road for contactless, controlled neuroregenerative therapies. An in vitro demonstration on the effect of ultrasonically stimulated piezoelectric β-PVDF for neurite generation in PC12 cells was provided by Hoop et al.[116] Commercially purchased PVDF membrane was coated with gold electrodes, and then actuated by ultrasonic waves to cause mechanical deformations (Figure 7q). The results showed that the ultrasound is capable of inducing polarization in the piezoelectric polymers, hence, initiating differentiation of PC12 cells (Figure 7r). This study demonstrates that using a combination of ultrasonic actuation and piezoelectric polymers is promising for the differentiation of neuronal cells and deserves further investigation.

Recent developments in tissue engineering have shown the application of PVDF scaffolds to preserve the contractility of cardiomyocytes and promote cell–cell communication.[117] In this study, the proposed scaffold is based on a polycaprolactone (PCL) magnetic nanofilm (MNF) coated with piezoelectric microfibers of PVDF–TrFE (PIEZO). To fabricate MNF+PIEZO scaffold, electrospun nanofibers of PIEZO deposited in a spin-coated solution of PCL. Piezoresponse force microscopy (PFM) shows the maximum piezoelectric constant of $d_{14} = 11.1$ pm V^{-1}. The reported results indicate that cardiac cells cultured in MNF+PIEZO scaffold have higher contractility for at least 12 days. Overall, the scaffold promotes rat and human cardiac cell attachment but future studies should further investigate the effect of piezoelectric materials in cardiomyocyte function.

PLLA: Tajitsu et al. in a series of papers[118–121] utilized the piezoelectric properties of PLLA to develop a biodegradable tweezer which can be inserted into the body through a catheter for the treatment of thrombosis. **Figure 8**a illustrates the operating principle of this simple tweezer. The PLLA fibers obtained by dry jet spinning were actuated by an externally applied AC voltage. The PLLA tweezer was then inserted into a blood vessel to demonstrate its ability to grasp a blockage due to thrombosis (Figure 8b–d), and then remove it (Figure 8e–g). The tweezer also demonstrated its potential to release and grasp a silica bead (Figure 8h,i). Due to the biocompatibility, biodegradability, and high sensitivity of the PLLA tweezers, PLLA will find applications in cellular biology, tissue engineering, nanomedicine, and cell delivery.

There are also numerous attempts to use the biocompatible and biodegradable piezoelectric PLLA polymer as a tissue stimulator to promote the proliferation and differentiation of cells. Implanted drawn (piezoelectric) PLLA rods in the intramedullary cavity of feline tibiae of cats form meaningfully higher callus in contrast to undrawn (non-piezoelectric) PLLA rods (Figure 8j,k).[122] As the draw ratio of the PLLA rod increased, fracture healing is clearly improved due to the increased callus formation. This finding strongly suggests that the drawn PLLA can provide improved fracture fixation devices, because they are resorbable in the body, making a second surgery unnecessary.

The fact that tissue regeneration benefits from the use of piezoelectric PLLA might be because polarized PLLA shows greater protein adsorption and enhances cellular adhesion and proliferation.[123,124] Figure 8l depicts a PFM image of nonpoled, positively poled, and negatively poled PLLA films. Figure 8m–p

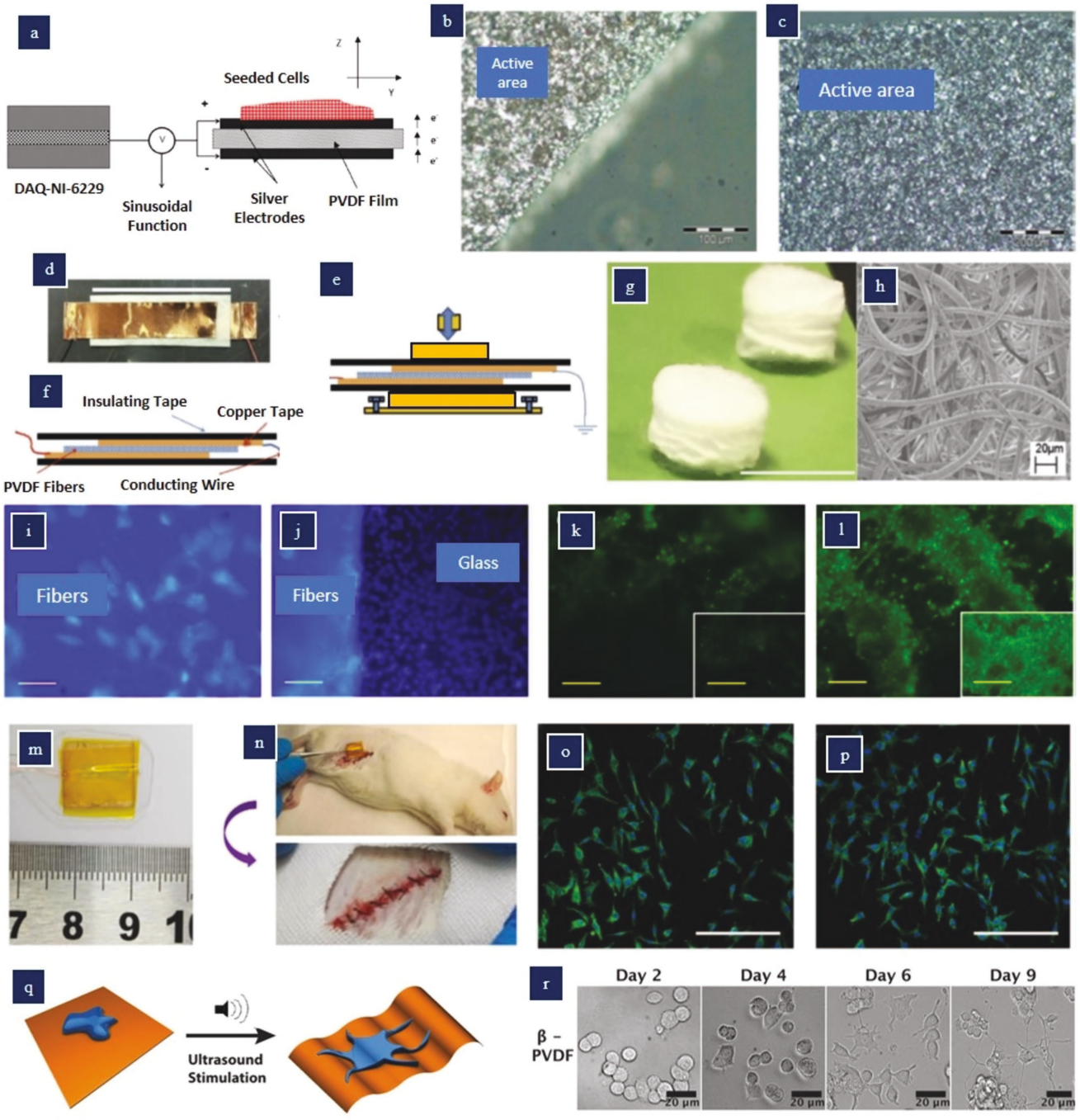

Figure 7. PVDF-based actuators and tissue stimulators. a) This scheme illustrated the cell culture exposition to micro vibration when seed in the active area of the piezoelectric subtract. b,c) Optical microscopy images that shows the distribution of the PMMA/bone-like apatite layer in the PVDF membrane. a–c) Reproduced with permission.[111] Copyright 2010, Elsevier. d) Top-down view of the electrical testing setup where the piezoelectric material is sandwiched between copper tape. e) Side-view and f) schematic of the testing device where force is applied and recording made by the oscilloscope. g) SEM images of the as-spun PVDF–TrFE. h) Annealed PVDF–TrFE. d–h) Reproduced with permission.[113] Copyright 2017, Elsevier. i–l) Panel showing in vitro interaction of cells with BTNP/PVDF under fluorescence microscopy: (i) microscopy image showing cell nuclei in the fibers, (j) microscopy image displaying many cell nuclei on the glass around the fibers, (k) conventional culture (static culture), and (l) bioreactor culture (dynamic culture). i–l) Reproduced with permission.[114] Copyright 2017, Elsevier. m) Image of electrospun PVDF–TrFE nanofiber scaffolds before implantation. n) The demonstration process of implanting the actuator in the subcutaneous thigh region of a Sprague Dawley (SD) rat (upper right) and the implanting site after suturing (lower right). o) Fluorescence microscopy images of L929 fibroblast cells on excited unpoled PVDF–TrFE and p) excited poled PVDF–TrFE scaffolds after 3 days. m–p) Reproduced with permission.[115] Copyright 2018, Elsevier. q) Ultrasound (US) stimulation of the piezoelectric β-PVDF membrane induces neuronal differentiation of PC12 cells due to wireless, mechanical deformation of the β-PVDF membrane. r) Time-lapse images of PC12 cells stimulated by piezoelectric β-PVDF upon US stimulation. q,r) Reproduced with permission.[116] Copyright 2017, Nature Publishing Group.

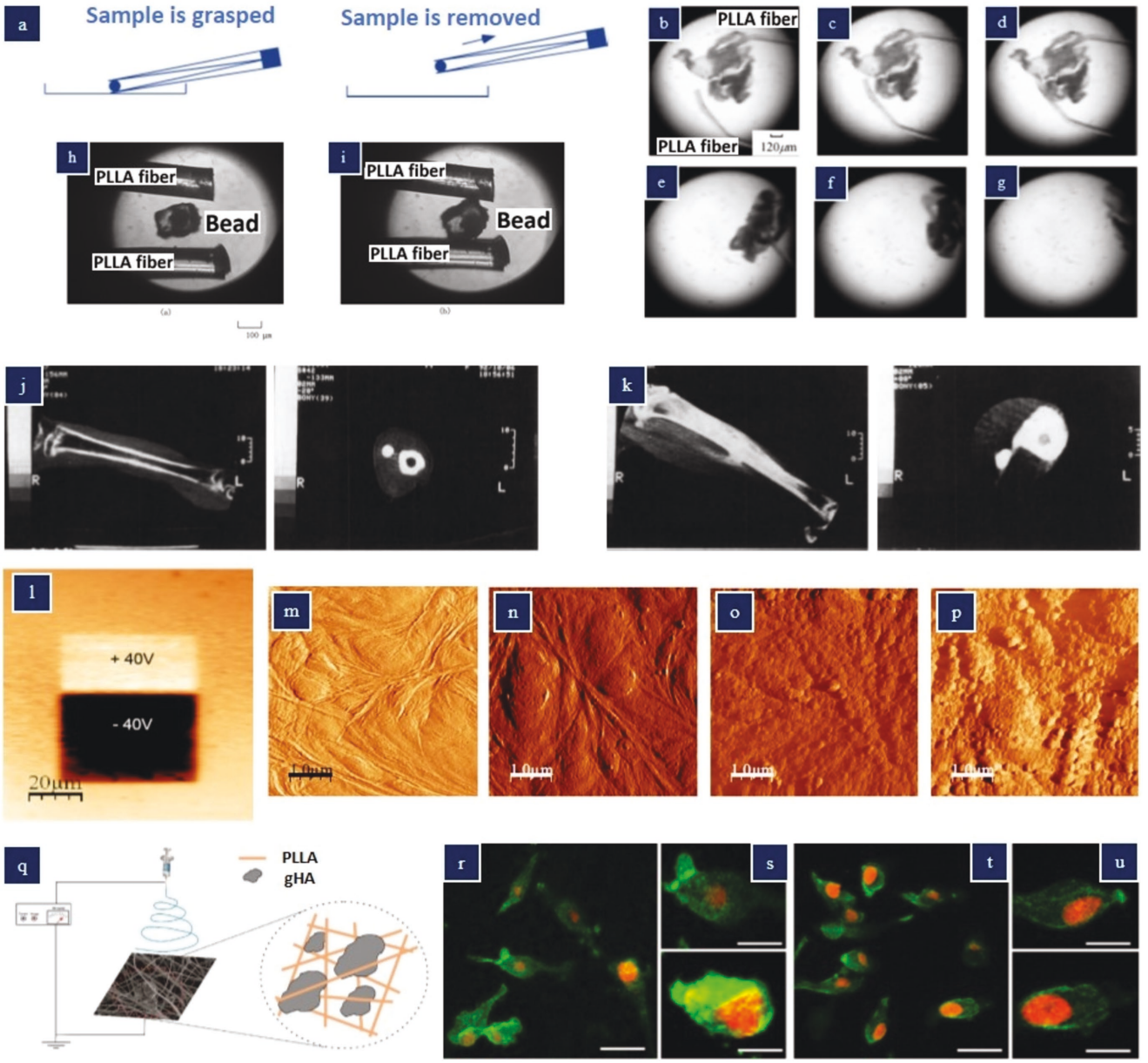

Figure 8. PLLA-based actuators and tissue stimulators. a) Schematic of demonstration of tweezers. b–d) Photographs showing the grasping of a thrombosis sample using PLLA fibers controlled by applied voltage and e–g) removal of a thrombosis sample. a–g) Reproduced with permission.[119] Copyright 2005, Taylor & Francis Group. h) Releasing a bead and i) grasping a bead using PLLA fibers with control by applied voltage. h,i) Reproduced with permission.[120] Copyright 2004, Taylor & Francis Group. j,k) X-ray CT photographs of the tibiae of cats at 8 weeks after implantation of rods of different materials: (j) undrawn PLLA, (k) drawn PLLA (draw ratio = 4). j,k) Reproduced with permission.[122] Copyright 1996, Wiley-VCH. l) Images of PLLA films obtained after poling with a DC bias of ±40 V. m–p) Topography images of PLLA thin film surfaces acquired in AFM tapping mode in liquid (m) nonpoled area before protein adsorption, (n) nonpoled area after protein adsorption, (o) positively poled area after protein adsorption, and (p) negatively poled area after protein adsorption. l–p) Reproduced with permission.[124] Copyright 2011, AIP Publishing LLC. q) Illustration of the fabrication electrospinning setup used to obtain the gHA–PLLA membranes. r–u) Confocal laser scanning microscopy (CLSM) representative images of MG-63 osteoblastic cells cultured on PLLA (r,s) and gHA–PLLA membranes (t,u) for 24 h. q–u) Reproduced with permission.[125] Copyright 2017, Elsevier.

illustrates the atomic force microscopy (AFM) results for four different PLLA films. It is obvious that a significantly higher quantity of proteins is adsorbed on the surface of the poled PLLA samples. Specifically, higher adhesion and proliferation of cells was observed in negatively charged PLLA. The protein adsorption test showed that surface charges can alter the conformation or orientation of the adsorbed proteins, which may expose or hinder their cell-binding domains.

Santos et al.[125] produced hybrid microcomposite electrospun membranes using PLLA as a matrix and glass-reinforced hydroxyapatite granules (gHA) micrometer particles as a filler material to increase bone regeneration compared to PLLA

membranes. It is important to note that electrospinning PLLA nanofibers have been shown to be piezoelectric (Figure 1d). The electrospinning setup used to obtain the PLLA and gHA–PLLA membranes is presented in Figure 8q. Osteoblastic cells were seeded on the composite membranes, and at day 1, an increased cell spreading was verified on the gHA–PLLA samples compared to the PLLA samples (Figure 8r–u). Bone-bonding ability showed that both the samples induced HA crystal nucleation, but gHA microcomposite allows a better F-actin cytoskeleton organization and increases alkaline phosphatase activity, making them potential candidates for bone healing applications.

4. Conclusion and Future Outlook

In summary, piezoelectric biomaterials are a class of functional materials that can convert mechanical deformation into electricity and vice versa. Those materials are or can be biocompatible for use in many different biodevices. We have reviewed the working principle of the different types of piezoelectric biomaterials used in biosensors, bioactuators, and tissue stimulators. State-of-the-art biocompatible piezoelectric materials have been reported with a focus on material properties. A comparison between the different piezoelectric biomaterials including organic and inorganic piezoelectric biomaterials has also been presented. Each of these materials must be chosen based on the application, and further developments are needed to transform them into useful biomedical devices. While inorganic piezoelectric materials have been widely explored, organic piezoelectric biomaterials offer a unique choice, particularly in biosensing applications owing to their excellent properties of being mechanically flexible and biocompatible.

Several challenges need to be overcome for better use of both inorganic piezoelectric and organic piezoelectric in medicine. These include 1) how to make highly efficient piezoelectric inorganics (such as PZT) more biocompatible, 2) how to improve modest piezoelectric constants of organic materials, and 3) how to obtain a robust control over dissolution rate of some biodegradable piezoelectric polymers (e.g., PLLA, silk, etc.). Solutions to the first problem include the use of biocompatible encapsulators or fabricating lead-free piezoelectric inorganics.[126–128] For the second problem, piezoelectricity in organic polymers can be enhanced by creating composites, mixing together organic and inorganic materials, or creating multilayer piezoelectric devices.[129–131] To solve the third challenge, biodegradable piezoelectric polymers can be treated under different conditions (e.g., different temperatures or stretching ratios or poling electrical fields) which will help to engineer their degradation rate.[132–134]

Despite such challenges, the field of piezoelectric biomaterials is gaining interest at a fast pace with growing applications in the development of biosensors and other biomedical devices. Recent advances in piezoelectric biomaterials and manufacturing/processing will continue to bring about new diagnostic tools and more effective treatments in medicine.

Conflict of Interest

The authors declare no conflict of interest.

Keywords

bioactuators, biodevices, biomaterials, biosensors, piezoelectricity

Received: March 31, 2018
Revised: July 1, 2018
Published online: October 8, 2018

[1] https://www.nature.com/subjects/biomaterials (accessed: June 2018).
[2] D. W. Hutmacher, *Biomaterials* **2000**, *21*, 2529.
[3] B.-S. Kim, D. J. Mooney, *Trends Biotechnol.* **1998**, *16*, 224.
[4] J. S. Temenoff, A. G. Mikos, *Biomaterials* **2000**, *21*, 2405.
[5] B. Yu, N. Long, Y. Moussy, F. Moussy, *Biosens. Bioelectron.* **2006**, *21*, 2275.
[6] P.-J. Chen, S. Saati, R. Varma, M. S. Humayun, Y.-C. Tai, *J. Microelectromech. Syst.* **2010**, *19*, 721.
[7] P. E. Daddona, G. T. Fieldson, A. S. Nat, W.-Q. Lin, *US Patent 6,091,975*, **2000**.
[8] H. Park, K. Park, *Pharm. Res.* **1996**, *13*, 1770.
[9] G. Voskerician, M. S. Shive, R. S. Shawgo, H. Von Recum, J. M. Anderson, M. J. Cima, R. Langer, *Biomaterials* **2003**, *24*, 1959.
[10] M. Vallet-Regí, F. Balas, D. Arcos, *Angew. Chem., Int. Ed.* **2007**, *46*, 7548.
[11] K. S. Ramadan, D. Sameoto, S. Evoy, *Smart Mater. Struct.* **2014**, *23*, 033001.
[12] J. S. Harrison, Z. Ounaies, in *Encyclopedia of Polymer Science and Technology*, John Wiley and Sons, New York **2002**, https://doi.org/10.1002/0471440264.pst427.
[13] A. H. Rajabi, M. Jaffe, T. L. Arinzeh, *Acta Biomater.* **2015**, *24*, 12.
[14] C. Ribeiro, V. Sencadas, D. M. Correia, S. Lanceros-Méndez, *Colloids Surf., B* **2015**, *136*, 46.
[15] Y. Qi, T. D. Nguyen, P. K. Purohit, M. C. McAlpine, in *Stretchable Electronics* (Ed: T. Someya), Wiley-VCH, Weinheim, Germany, **2012**, Ch. 5, p. 111.
[16] J. Nathan, K. Lynette, M. Alan, *Smart Mater. Struct.* **2013**, *22*, 115033.
[17] C. Dagdeviren, S.-W. Hwang, Y. Su, S. Kim, H. Cheng, O. Gur, R. Haney, F. G. Omenetto, Y. Huang, J. A. Rogers, *Small* **2013**, *9*, 3398.
[18] C. K. Jeong, I. Kim, K.-I. Park, M. H. Oh, H. Paik, G.-T. Hwang, K. No, Y. S. Nam, K. J. Lee, *ACS Nano* **2013**, *7*, 11016.
[19] Y. Wang, X. Y. Zhou, Z. Chen, B. Cai, Z. Z. Ye, C. Y. Gao, J. Y. Huang, *Appl. Phys. A: Solids Surf.* **2014**, *117*, 2121.
[20] J. Wilson, G. H. Pigott, F. J. Schoen, L. L. Hench, *J. Biomed. Mater. Res.* **1981**, *15*, 805.
[21] *Soft Actuators: Materials, Modeling, Applications, and Future Perspectives* (Eds: K. Asaka, H. Okuzaki), Springer, Tokyo, Japan **2014**.
[22] M. Yoshida, A. Masanobu, G. Kenichi, F. Ichiro, I. Takaharu, O. Takayuki, T. Yoshiro, U. Shinichi, K. Takeshi, A. Yoshiaki, *US Patent 8,648,151*, **2014**.
[23] E. Fukada, *Biorheology* **1995**, *32*, 593.
[24] K. Ohnuma, *US Patent Application 13/890,573*, **2013**.
[25] S. Lang, S. Tofail, A. Kholkin, M. Wojtaś, M. Gregor, A. Gandhi, Y. Wang, S. Bauer, M. Krause, A. Plecenik, *Sci. Rep.* **2013**, *3*, 2215.
[26] Y. Q. Fu, J. K. Luo, N.-T. Nguyen, A. J. Walton, A. J. Flewitt, X.-T. Zu, Y. Li, G. McHale, A. Matthews, E. Iborra, H. Du, W. I. Milne, *Prog. Mater. Sci.* **2017**, *89*, 31.
[27] M. Que, R. Zhou, X. Wang, Z. Yuan, G. Hu, C. Pan, *J. Phys.: Condens. Matter* **2016**, *28*, 433001.
[28] W.-C. Shih, Y.-C. Chen, W.-T. Chang, C.-C. Cheng, P.-C. Liao, K.-S. Kao, *J. Nanomater.* **2014**, *2014*, 2.

[29] L. Swallow, J. Luo, E. Siores, I. Patel, D. Dodds, *Smart Mater. Struct.* **2008**, *17*, 025017.
[30] D. Paul, A. Roy, *Int. J. Eng. Tech. Res.* **2015**, *3*, 2321.
[31] K. Cung, B. J. Han, T. D. Nguyen, S. Mao, Y.-W. Yeh, S. Xu, R. R. Naik, G. Poirier, N. Yao, P. K. Purohit, *Nano Lett.* **2013**, *13*, 6197.
[32] Y. Zang, F. Zhang, C.-a. Di, D. Zhu, *Mater. Horiz.* **2015**, *2*, 140.
[33] R. Bao, C. Wang, L. Dong, R. Yu, K. Zhao, Z. L. Wang, C. Pan, *Adv. Funct. Mater.* **2015**, *25*, 2884.
[34] C. Pan, L. Dong, G. Zhu, S. Niu, R. Yu, Q. Yang, Y. Liu, Z. L. Wang, *Nat. Photonics* **2013**, *7*, 752.
[35] M. Jaishankar, T. Tseten, N. Anbalagan, B. B. Mathew, K. N. Beeregowda, *Interdiscip. Toxicol.* **2014**, *7*, 60.
[36] T. Sakai, S. Hoshiai, E. Nakamachi, *J. Optoelectron. Adv. Mater.* **2006**, *8*, 1435.
[37] Q. Wei, *Surface Modification of Textiles*, Woodhead Publishing **2009**.
[38] A. Janotti, C. G. Van de Walle, *Rep. Prog. Phys.* **2009**, *72*, 126501.
[39] Y. Zhang, T. R Nayak, H. Hong, W. Cai, *Curr. Mol. Med.* **2013**, *13*, 1633.
[40] Y. Chu, L. Wan, G. Ding, P. Wu, D. Qiu, J. Pan, H. He, in *2013 14th Int. Conf. on Electronic Packaging Technology (ICEPT)* (Eds: K. Bi, M. Huang, N. Zhao), IEEE, Piscataway, NJ, USA **2013**.
[41] J. Lu, L. Zhang, H. Takagi, T. Itoh, R. Maeda, *J. Appl. Sci. Eng.* **2014**, *17*, 17r24.
[42] R. Kumar, O. Al-Dossary, G. Kumar, A. Umar, *Nano-Micro Lett.* **2015**, *7*, 97.
[43] S. A. Jewett, M. S. Makowski, B. Andrews, M. J. Manfra, A. Ivanisevic, *Acta Biomater.* **2012**, *8*, 728.
[44] W.-S. Jung, *Mater. Lett.* **2002**, *57*, 110.
[45] G. Meneghesso, G. Verzellesi, F. Danesin, F. Rampazzo, F. Zanon, A. Tazzoli, M. Meneghini, E. Zanoni, *IEEE Trans. Device Mater. Reliab.* **2008**, *8*, 332.
[46] J. Guo, F. Pan, M. Feng, R. Guo, P. Chou, C. Chang, *J. Appl. Phys.* **1996**, *80*, 1623.
[47] S. Gupta, M. Elias, X. Wen, J. Shapiro, L. Brillson, W. Lu, S. C. Lee, *Biosens. Bioelectron.* **2008**, *24*, 505.
[48] M. Hofstetter, J. Howgate, M. Schmid, S. Schoell, M. Sachsenhauser, D. Adigüzel, M. Stutzmann, I. D. Sharp, S. Thalhammer, *Biochem. Biophys. Res. Commun.* **2012**, *424*, 348.
[49] Q. Li, Q. Wang, *Macromol. Chem. Phys.* **2016**, *217*, 1228.
[50] C. Wan, C. R. Bowen, *J. Mater. Chem. A* **2017**, *5*, 3091.
[51] V. S. Bystrov, E. V. Paramonova, I. K. Bdikin, A. V. Bystrova, R. C. Pullar, A. L. Kholkin, *J. Mol. Model.* **2013**, *19*, 3591.
[52] K. Uchino, *Ultrasonic Transducers: Materials and Design for Sensors, Actuators and Medical Applications*, 1st ed. (Ed: K. Nakamura), Elsevier, New York **2012**, p. 70.
[53] H.-F. Guo, Z.-S. Li, S.-W. Dong, W.-J. Chen, L. Deng, Y.-F. Wang, D.-J. Ying, *Colloids Surf., B* **2012**, *96*, 29.
[54] N. Fadhil, D. Saber, P. Cox, K. Vanashi, P. Patra, in *American Society for Engineering Education Zone 1 Conference at the University of Bridgeport*, American Society for Engineering Education, Washington, DC, USA **2014**.
[55] Z.-M. Dang, L.-Z. Fan, Y. Shen, C.-W. Nan, *Mater. Sci. Eng., B* **2003**, *103*, 140.
[56] A. Kono, K. Shimizu, H. Nakano, Y. Goto, Y. Kobayashi, T. Ougizawa, H. Horibe, *Polymer* **2012**, *53*, 1760.
[57] A. Sultana, S. K. Ghosh, V. Sencadas, T. Zheng, M. J. Higgins, T. R. Middya, D. Mandal, *J. Mater. Chem. B* **2017**, *5*, 7352.
[58] T. Yoshida, K. Imoto, K. Tahara, K. Naka, Y. Uehara, S. Kataoka, M. Date, E. Fukada, Y. Tajitsu, *Jpn. J. Appl. Phys.* **2010**, *49*, 09MC11.
[59] T. Ochiai, E. Fukada, *Jpn. J. Appl. Phys.* **1998**, *37*, 3374.
[60] S. Trolier-McKinstry, P. Muralt, *J. Electroceram.* **2004**, *12*, 7.
[61] S. Priya, H.-C. Song, Y. Zhou, R. Varghese, A. Chopra, S.-G. Kim, I. Kanno, L. Wu, D. S. Ha, J. Ryu, *Energy Harvesting Syst.* **2017**, *4*, 3.
[62] Y. Iitaka, *Nature* **1959**, *183*, 390.
[63] S. Guerin, A. Stapleton, D. Chovan, R. Mouras, M. Gleeson, C. McKeown, M. R. Noor, C. Silien, F. M. Rhen, A. L. Kholkin, N. Liu, T. Soulimane, S. A. M. Tofail, D. Thompson, *Nat. Mater.* **2018**, *17*, 180.
[64] D. Isakov, E. de Matos Gomes, I. Bdikin, B. Almeida, M. Belsley, M. Costa, V. Rodrigues, A. Heredia, *Cryst. Growth Des.* **2011**, *11*, 4288.
[65] Z. Zhou, D. Qian, M. Minary-Jolandan, *ACS Biomater. Sci. Eng.* **2016**, *2*, 929.
[66] M. Minary-Jolandan, M.-F. Yu, *Nanotechnology* **2009**, *20*, 085706.
[67] C. Silva, C. Lima, A. Pinheiro, J. Goes, S. Figueiro, A. Sombra, *Phys. Chem. Chem. Phys.* **2001**, *3*, 4154.
[68] D. Denning, M. Paukshto, S. Habelitz, B. J. Rodriguez, *J. Biomed. Mater. Res., Part B* **2014**, *102*, 284.
[69] J. Joseph, S. G. Singh, S. R. K. Vanjari, *IEEE Sens. J.* **2017**, *17*, 8306.
[70] T. Yucel, P. Cebe, D. L. Kaplan, *Adv. Funct. Mater.* **2011**, *21*, 779.
[71] Y. Wang, H.-J. Kim, G. Vunjak-Novakovic, D. L. Kaplan, *Biomaterials* **2006**, *27*, 6064.
[72] Y. Yang, F. Ding, J. Wu, W. Hu, W. Liu, J. Liu, X. Gu, *Biomaterials* **2007**, *28*, 5526.
[73] L. Meinel, O. Betz, R. Fajardo, S. Hofmann, A. Nazarian, E. Cory, M. Hilbe, J. McCool, R. Langer, G. Vunjak-Novakovic, *Bone* **2006**, *39*, 922.
[74] A. Kholkin, N. Amdursky, I. Bdikin, E. Gazit, G. Rosenman, *ACS Nano* **2010**, *4*, 610.
[75] E. Bosne, A. Heredia, S. Kopyl, D. Karpinsky, A. Pinto, A. Kholkin, *Appl. Phys. Lett.* **2013**, *102*, 073504.
[76] S. J. Heerema, C. Dekker, *Nat. Nanotechnol.* **2016**, *11*, 127.
[77] S. Xu, J. Zhan, B. Man, S. Jiang, W. Yue, S. Gao, C. Guo, H. Liu, Z. Li, J. Wang, *Nat. Commun.* **2017**, *8*, 14902.
[78] G. S. Kulkarni, K. Reddy, Z. Zhong, X. Fan, *Nat. Commun.* **2014**, *5*, 4376.
[79] G. da Cunha Rodrigues, P. Zelenovskiy, K. Romanyuk, S. Luchkin, Y. Kopelevich, A. Kholkin, *Nat. Commun.* **2015**, *6*, 7572.
[80] Y.-M. You, W.-Q. Liao, D. Zhao, H.-Y. Ye, Y. Zhang, Q. Zhou, X. Niu, J. Wang, P.-F. Li, D.-W. Fu, *Science* **2017**, *357*, 306.
[81] A. S. Dahiya, F. Morini, S. Boubenia, K. Nadaud, D. Alquier, G. Poulin-Vittrant, *Adv. Mater. Technol.* **2018**, *3*, 1700249.
[82] M. Lee, C. Y. Chen, S. Wang, S. N. Cha, Y. J. Park, J. M. Kim, L. J. Chou, Z. L. Wang, *Adv. Mater.* **2012**, *24*, 1759.
[83] Y. Hu, C. Xu, Y. Zhang, L. Lin, R. L. Snyder, Z. L. Wang, *Adv. Mater.* **2011**, *23*, 4068.
[84] V. Bystrov, I. Bdikin, A. Heredia, R. Pullar, E. Mishina, A. Sigov, A. Kholkin, *Piezoelectric Nanomaterials for Biomedical Applications*, Springer, New York **2012**.
[85] I. Guy, S. Muensit, E. Goldys, *Appl. Phys. Lett.* **1999**, *75*, 4133.
[86] R. E. Newnham, *Properties of Materials: Anisotropy, Symmetry, Structure*, Oxford University Press, New York **2005**.
[87] *Stretchable Electronics* (Ed: T. Someya), Wiley-VCH, Weinheim, Germany **2013**.
[88] Y. Tajitsu, *IEEE Transactions on Ultrasonics, Ferroelectrics, and Frequency Control*, *Vol*. 55, IEEE, Piscataway, NJ, USA **2008**, p. 55.
[89] C. Dagdeviren, Y. Shi, P. Joe, R. Ghaffari, G. Balooch, K. Usgaonkar, O. Gur, P. L. Tran, J. R. Crosby, M. Meyer, *Nat. Mater.* **2015**, *14*, 728.
[90] T. D. Nguyen, N. Deshmukh, J. M. Nagarah, T. Kramer, P. K. Purohit, M. J. Berry, M. C. McAlpine, *Nat. Nanotechnol.* **2012**, *7*, 587.
[91] C. Dagdeviren, B. D. Yang, Y. Su, P. L. Tran, P. Joe, E. Anderson, J. Xia, V. Doraiswamy, B. Dehdashti, X. Feng, *Proc. Natl. Acad. Sci. USA* **2014**, *111*, 1927.
[92] G. T. Hwang, H. Park, J. H. Lee, S. Oh, K. I. Park, M. Byun, H. Park, G. Ahn, C. K. Jeong, K. No, *Adv. Mater.* **2014**, *26*, 4880.
[93] G. Zhu, A. C. Wang, Y. Liu, Y. Zhou, Z. L. Wang, *Nano Lett.* **2012**, *12*, 3086.

[94] P. Rajagopalan, V. Singh, I. Palani, *Nanotechnology* **2018**, *29*, 105406.
[95] N. Jamond, P. Chrétien, L. Gatilova, E. Galopin, L. Travers, J.-C. Harmand, F. Glas, F. Houzé, N. Gogneau, *Nanoscale* **2017**, *9*, 4610.
[96] S.-J. Tsai, C.-L. Wu, N.-T. Tsai, S.-S. Wong, L.-W. Tu, *Carbon* **2018**, *130*, 390.
[97] D. Cannatà, M. Benetti, E. Verona, A. Varriale, M. Staiano, S. D'Auria, F. Di Pietrantonio, in *2012 IEEE Int. Ultrasonics Symp. (IUS)*, IEEE, Piscataway, NJ, USA **2012**.
[98] D. Chen, J. Wang, Y. Xu, *IEEE Sens. J.* **2013**, *13*, 2217.
[99] L. Persano, C. Dagdeviren, Y. Su, Y. Zhang, S. Girardo, D. Pisignano, Y. Huang, J. A. Rogers, *Nat. Commun.* **2013**, *4*, 1633.
[100] E. J. Curry, K. Ke, M. T. Chorsi, K. S. Wrobel, A. N. Miller, A. Patel, I. Kim, J. Feng, L. Yue, Q. Wu, C.-L. Kuo, K. W.-H. Lo, C. T. Laurencin, H. Ilies, P. K. Purohit, T. D. Nguyen, *Proc. Natl. Acad. Sci. USA* **2018**, *115*, 909.
[101] C. Li, P.-M. Wu, L. A. Shutter, R. K. Narayan, *Appl. Phys. Lett.* **2010**, *96*, 053502.
[102] T. Sharma, S.-S. Je, B. Gill, J. X. Zhang, *Sens. Actuators, A* **2012**, *177*, 87.
[103] T. Sharma, K. Aroom, S. Naik, B. Gill, J. X. Zhang, *Ann. Biomed. Eng.* **2013**, *41*, 744.
[104] C. Li, P.-M. Wu, S. Lee, A. Gorton, M. J. Schulz, C. H. Ahn, *J. Microelectromech. Syst.* **2008**, *17*, 334.
[105] T. Sharma, J. Langevine, S. Naik, K. Aroom, B. Gill, J. X. Zhang, in *2013 Transducers & Eurosensors XXVII: The 17th Int. Conf. on Solid-State Sensors, Actuators and Microsystems (TRANSDUCERS & EUROSENSORS XXVII)*, IEEE, Piscataway, NJ, USA **2013**.
[106] Z. Liu, S. Zhang, Y. Jin, H. Ouyang, Y. Zou, X. Wang, L. Xie, Z. Li, *Semicond. Sci. Technol.* **2017**, *32*, 064004.
[107] X. Wang, Y. Gu, Z. Xiong, Z. Cui, T. Zhang, *Adv. Mater.* **2014**, *26*, 1336.
[108] S. K. Ghosh, D. Mandal, *ACS Sustainable Chem. Eng.* **2017**, *5*, 8836.
[109] S. Moreno, M. Baniasadi, S. Mohammed, I. Mejia, Y. Chen, M. A. Quevedo-Lopez, N. Kumar, S. Dimitrijevich, M. Minary-Jolandan, *Adv. Electron. Mater.* **2015**, *1*, 1500154.
[110] J. Park, M. Kim, Y. Lee, H. S. Lee, H. Ko, *Sci. Adv.* **2015**, *1*, e1500661.
[111] C. Frias, J. Reis, F. Capela e Silva, J. Potes, J. Simões, A. Marques, *Compos. Sci. Technol.* **2010**, *70*, 1920.
[112] C. Frias, J. Reis, F. Capela e Silva, J. Potes, J. Simões, A. Marques, *J. Biomech.* **2010**, *43*, 1061.
[113] S. M. Damaraju, Y. Shen, E. Elele, B. Khusid, A. Eshghinejad, J. Li, M. Jaffe, T. L. Arinzeh, *Biomaterials* **2017**, *149*, 51.
[114] C. Mota, M. Labardi, L. Trombi, L. Astolfi, M. D'Acunto, D. Puppi, G. Gallone, F. Chiellini, S. Berrettini, L. Bruschini, *Mater. Des.* **2017**, *122*, 206.
[115] A. Wang, Z. Liu, M. Hu, C. Wang, X. Zhang, B. Shi, Y. Fan, Y. Cui, Z. Li, K. Ren, *Nano Energy* **2018**, *43*, 63.
[116] M. Hoop, X.-Z. Chen, A. Ferrari, F. Mushtaq, G. Ghazaryan, T. Tervoort, D. Poulikakos, B. Nelson, S. Pané, *Sci. Rep.* **2017**, *7*, 4028.
[117] P. J. Gouveia, S. Rosa, L. Ricotti, B. Abecasis, H. Almeida, L. Monteiro, J. Nunes, F. S. Carvalho, M. Serra, S. Luchkin, *Biomaterials* **2017**, *139*, 213.
[118] Y. Tajitsu, *Polym. Adv. Technol.* **2006**, *17*, 907.
[119] Y. Tajitsu, M. Kanesaki, M. Tsukiji, K. Imoto, M. Date, E. Fukada, *Ferroelectrics* **2005**, *320*, 133.
[120] Y. Tajitsu, S. Kawai, M. Kanesaki, M. Date, E. Fukada, *Ferroelectrics* **2004**, *304*, 195.
[121] M. Sawano, K. Tahara, Y. Orita, M. Nakayama, Y. Tajitsu, *Polym. Int.* **2010**, *59*, 365.
[122] Y. Ikada, Y. Shikinami, Y. Hara, M. Tagawa, E. Fukada, *J. Biomed. Mater. Res., Part A* **1996**, *30*, 553.
[123] N. Barroca, A. Daniel-da-Silva, P. Gomes, M. Fernandes, S. Lanceros-Méndez, P. Sharma, A. Gruverman, M. Fernandes, P. Vilarinho, *Microsc. Microanal.* **2012**, *18*, 63.
[124] N. Barroca, P. M. Vilarinho, A. L. Daniel-da-Silva, A. Wu, M. H. Fernandes, A. Gruverman, *Appl. Phys. Lett.* **2011**, *98*, 133705.
[125] D. Santos, D. M. Silva, P. S. Gomes, M. H. Fernandes, J. D. Santos, V. Sencadas, *J. Colloid Interface Sci.* **2017**, *504*, 101.
[126] D. B. Deutz, N. T. Mascarenhas, J. B. J. Schelen, D. M. de Leeuw, S. van der Zwaag, P. Groen, *Adv. Funct. Mater.* **2017**, *27*, 1700728.
[127] D. H. Kim, T. G. Lee, S. H. Cho, K. T. Lee, C. Y. Kang, W. K. Lee, S. Nahm, *J. Am. Ceram. Soc.* **2017**, *100*, 5367.
[128] H. Yokozawa, Y. Doshida, S. Kishimoto, T. Morita, *Sens. Actuators, A* **2018**, *274*, 179.
[129] Z. Xu, J. Bykova, M. Baniasadi, S. Moreno, Z. Zhou, N. Das, S. Bandi, Y. Xi, D. Qian, R. H. Baughman, M. Minary-Jolandan, *Adv. Eng. Mater.* **2017**, *19*, 1600570.
[130] M. Chatzinikolaidou, S. Rekstyte, P. Danilevicius, C. Pontikoglou, H. Papadaki, M. Farsari, M. Vamvakaki, *Mater. Sci. Eng., C* **2015**, *48*, 301.
[131] Y. W. Kim, H. B. Lee, S.-M. Yeon, J. H. Park, H. J. Lee, J. Yoon, S. H. Park, *ACS Appl. Mater. Interfaces* **2018**, *10*, 5723.
[132] Z. Guo, D. Bo, P. He, H. Li, G. Wu, Z. Li, C. Zhou, Q. Li, *J. Mater. Chem. B* **2017**, *5*, 7701.
[133] Y. Kikkawa, S. Tanaka, Y. Norikane, *RSC Adv.* **2017**, *7*, 55720.
[134] S. S. Surwase, N. M. Munot, B. B. Idage, S. B. Idage, *Drug Delivery Transl. Res.* **2017**, *7*, 416.